Bioorganic & Medicinal Chemistry Letters 22 (2012) 4707–4712

Contents lists available at SciVerse ScienceDirect

Bioorganic & Medicinal Chemistry Letters

journal homepage: www.elsevier.com/locate/bmcl

Development and evaluation of multifunctional agents for potential treatment of Alzheimer's disease: Application to a pyrimidine-2,4-diamine template

Tarek Mohamed [a,b], Jacky C. K. Yeung [b], Maryam S. Vasefi [a,c], Michael A. Beazely [a], Praveen P. N. Rao [a,*]

[a] School of Pharmacy, Health Sciences Campus, University of Waterloo, Waterloo, Ontario, Canada N2L 3G1
[b] Department of Chemistry, University of Waterloo, Waterloo, Ontario, Canada N2L 3G1
[c] Department of Biology, University of Waterloo, Waterloo, Ontario, Canada N2L 3G1

ARTICLE INFO

Article history:
Received 5 May 2012
Revised 18 May 2012
Accepted 18 May 2012
Available online 26 May 2012

ABSTRACT

We investigated a group of 2-benzylpiperidin-*N*-benzylpyrimidin-4-amines with various electron-withdrawing or electron-donating groups (EWGs or EDGs, respectively) as multi-targeted Alzheimer's disease (AD) therapeutics. The synthesized derivatives were screened for anti-cholinesterase (AChE and BuChE), anti-Aβ-aggregation (AChE- and self-induced) and anti-β-secretase (BACE-1) activities in an effort to identify lead, multifunctional candidates as part of our multi-targeted approach to treat AD. Biological assessment revealed that the nature of the substituent on the C-4 benzylamine group (e.g., halogen vs methoxy-based) greatly affected the biological profile. In vitro screening identified N^2-(1-benzylpiperidin-4-yl)-N^4-(3,4-dimethoxybenzyl)pyrimidine-2,4-diamine (**7h**) as the lead candidate with a dual ChE (AChE IC_{50} = 9.9 μM; BuChE IC_{50} = 11.4 μM), Aβ-aggregation (AChE-induced = 59.3%; self-induced = 17.4% at 100 μM) and BACE-1 (34% inhibition at 10 μM) inhibitory profile along with good cell viability (% neuroblastoma cell viability at 40 μM = 81.0%). Molecular modeling studies indicate that a central pyrimidine-2,4-diamine ring serves as a suitable template to develop novel small molecule candidates to target multiple pathological routes in AD.

Alzheimer's disease (AD) is a highly complex and rapidly progressive, neurodegenerative disease that manifests in the cholinergic branch of the central nervous system (CNS).[1] The hallmarks of AD include the rapid onset of cholinergic dysfunction, accelerated formation and aggregation of amyloid-β (Aβ) peptides, collapse of the neuronal cytoskeleton and formation of neurofibrillary tangles (NFTs) of hyperphosphorylated tau protein.[2–6] Its devastating pathology is jointly described by the cholinergic, amyloid and tau hypotheses, respectively, where the end result is neuronal cell death leading to the onset of dementia symptoms and eventually death. With an increase in the aging population, AD's prevalence amongst the elderly is on the rise.[2,3]

The cholinergic hypothesis describes AD pathology as a systemic collapse in cholinergic neurotransmission as a result of the overall decline in acetylcholine (ACh): a vital neurotransmitter utilized by sympathetic and parasympathetic neurons.[7] Cholinesterase (ChE isoforms: AChE and BuChE) enzymes act on ACh to terminate its actions in the synapse by degrading it to choline and acetate.[8,9] A shift in the ratio of AChE to BuChE has been observed and that seems to be dependent on the stage of the disease. In early pathogenesis, AChE is considered the primary degrading enzyme and therefore, it plays a vital role in disease progression; however, as neuronal cells are depleted and AChE concentrations fall, BuChE (the secondary ChE with a wider distribution within the body) acts as the major degrading enzyme.[10,11]

The amyloid hypothesis attributes the onset and progression of AD to the rapid generation and aggregation (metal-ion-promoted, self-promoted or AChE-promoted) of toxic amyloid-β (Aβ) peptides.[12–14] Amyloid precursor protein (APP) is normally processed by α-secretase, but with AD, a shift in APP processing occurs where β-secretase (BACE-1) takes over generating pro-A β domains subsequently processed by γ-secretase, leading to the liberation of $Aβ_{1-40/42}$ peptides.[12–14] Recent and ongoing research efforts have uncovered links between the cholinergic and amyloid hypotheses including a key role of AChE in promoting Aβ-aggregation leading to highly toxic AChE–Aβ peptide complexes as well as the role of acetycholine receptors (AChRs) in modulating the APP processing pathways.[15–19]

Collectively, these complex factors of AD pathology strengthen the necessity to develop multi-targeted/multifunctional therapies that could exhibit disease-modifying effects (DMEs) in an effort to reverse disease manifestation.[20]

Abbreviations: AD, Alzheimer's disease; ChEIs, cholinesterase inhibitors; *h*AChE, human acetylcholinesterase; *h*BuChE, human butyrylcholinesterase; *eq*BuChE, equinebutyrylcholinesterase; SAR, structure–activity relationship; Aβ, amyloid-β; DTNB, 5,5′-dithiobis(2-nitrobenzoic acid); ThT, thioflavin T; MTT, 3-(4,5-dimethylthiazol-2-yl)-2,5-diphenyl tetrazolium bromide; BACE-1, β-secretase or beta-site amyloid precursor protein cleaving enzyme.

* Corresponding author. Tel.: +1 519 888 4567x21317.
E-mail address: praopera@uwaterloo.ca (P.P.N. Rao).

0960-894X/$ - see front matter © 2012 Elsevier Ltd. All rights reserved.
http://dx.doi.org/10.1016/j.bmcl.2012.05.077

Currently marketed AD pharmacotherapies (Fig. 1) such as Aricept® (donepezil–**1**) and Razadyne® (galantamine–**2**) offer symptomatic relief, while the latter can be classified as a multifunctional agent as it targets the ChE enzymes along with enhancing nicotinic AChR activity and blocking Aβ-aggregation.[21,22] We previously reported the development of a group of heterocyclic, non-fused ChEIs based on a 2,4-disubstituted pyrimidine ring (2,4-DPR) template, where compounds **3** and **4** (Fig. 1) were identified as lead derivatives based on their ChE and Aβ-aggregation inhibition profiles.[23,24]

Here we report the development and evaluation of new heterocycles (**7a**–**j**) containing a pyrimidine-2,4-diamine scaffold as novel small molecules possessing multifunctional activity against the ChE enzymes, amyloid aggregation (both AChE and self-induced) and BACE-1.

The synthesis of target pyrimidine-2,4-diamine derivatives was accomplished in two steps. In the first step, various C-4 substituted benzyl-2-chloropyrimidin-4-amine intermediates (**6a**–**j**) were synthesized from the 2,4-dichloropyrimidine starting material (**5**) by a nucleophilic aromatic substitution reaction at C-4 using *N,N*-diisopropylethylamine (DIPEA) and appropriate benzylamine (R^1 = 2-chloro, 3-chloro, 4-chloro, 4-bromo, 4-fluoro, 4-methyl, 4-methoxy, 3,4-dimethoxy, 3,4,5-trimethoxybenzylamine and piperonylamine, respectively). The reaction was carried out in EtOH at 80–85 °C and refluxed for 4 h. Intermediates **6a**–**j** were obtained in moderate to good yield ranging from 60% to 89% (Scheme 1).[23–25]

In the second step, the C-2 chlorine was displaced by 4-amino-1-benzylpiperidine. This coupling reaction was run under vigorous conditions (190–195 °C) for 14–16 h with DIPEA in a sealed pressure vessel (PV) using *n*-BuOH as a solvent (Scheme 1). The target pyrimidine-2,4-diamine derivatives (**7a**–**j**) were obtained in moderate to good yields (45–54%) (Scheme 1).[23,24,26]

The ability of the synthesized derivatives (**7a**–**j**) to inhibit both ChEs (*h*AChE and *eq*BuChE), *h*AChE-induced and self-induced $A\beta_{1-40}$ aggregation as well as BACE-1 was evaluated in vitro (IC_{50} values or % inhibition at 100 μM, Tables 1 and 2).[23,24,27,28] The SAR studies indicated that the multifunctional capability of the pyrimidine-2,4-diamine derivatives was sensitive to steric and electronic properties at the C-2 and C-4 positions. They derivatives exhibited a broad range of inhibition (*h*AChE IC_{50} = 7.7 to 12.9 μM; *eq*BuChE IC_{50} = 2.2 to 11.4 μM; *h*AChE-induced $A\beta_{1-40}$ aggregation = inactive to 59.3%; self-induced $A\beta_{1-40}$ aggregation = inactive to 48.4% and BACE-1 IC_{50} range = 0.6 to >50 μM).

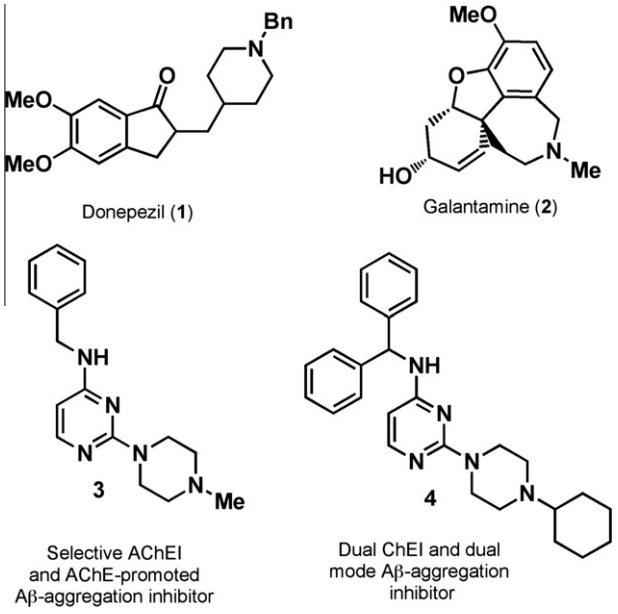

Fig. 1. Structures of some anti-AD agents (**1**–**4**).

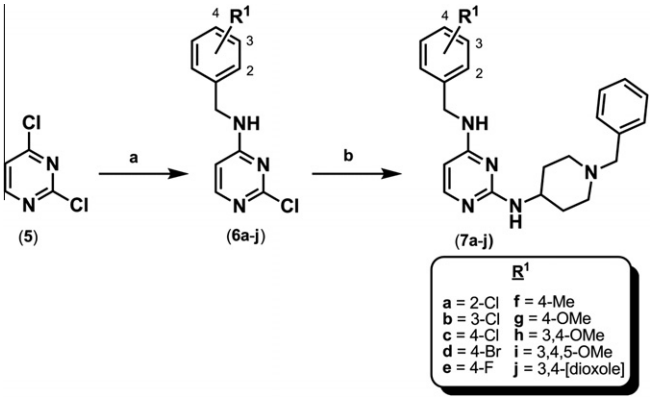

Scheme 1. Reagents and conditions: (a) DIPEA, primary amines (H_2N-R), EtOH, 0 °C to 85–90 °C and reflux for 4 h. (b) DIPEA, 4-amino-1-benzylpiperidine, *n*-BuOH, 190–195 °C, 14–16 h.

Based on molecular modeling studies, we incorporated a benzylpiperidine pharmacophore at C-2 position that is present in the donepezil in order to obtain dual AChE and BuChE inhibition whereas the C-4-position of the pyrimidine-2,4-diamine was varied to develop a suitable peripheral anionic site (PAS) binding pharmacophore (**7a–j**, Table 1). The C-4 halogen-substituted benzyl derivatives (**7a–e**) exhibited AChE inhibition with IC_{50} values ranging from 7.7 μM to 9.9 μM and BuChE inhibition with IC_{50} values ranging from 2.2 μM to 4.1 μM. The location of a chlorine (*ortho*, *meta* or *para*) on the C-4 benzyl substituent (**7a**, **7b** and **7c**) did not affect AChE or BuChE inhibition and potency to a great extent (AChE IC_{50} = 7.7–8.8 μM range; BuChE IC_{50} = 2.4–2.8 μM range). Interestingly, the replacement of the *p*-Cl with a *p*-F did not exhibit a significant change either (**7e**, AChE IC_{50} = 7.7 μM; BuChE IC_{50} = 2.2 μM) despite the differences in size and electronegativity. On the other hand, when a bromine halogen is placed at the *para* position, it results a slight decrease in AChE potency and almost twofold decrease in BuChE potency (**7d**, AChE IC_{50} = 9.9 μM; BuChE IC_{50} = 4.1 μM) compared to **7e**. All compounds from this series exhibited superior BuChE inhibition compared to reference agents donepezil (BuChE IC_{50} = 3.6 μM) and galantamine (BuChE IC_{50} = 12.6 μM, Table 1).

As a next step we explored the possibility of developing a suitable pharmacophore at C-4 position of the pyrimidine ring that could potentially bind to the PAS of AChE.[13,17] In this regard, the C-4 benzyl group was substituted with 3,4-dimethoxy, 3,4,5-trimethoxy and a fused ring (3,4-methylenedioxy) (**7f–j**, Table 1). These compounds were compared with 4-methyl and 4-methoxybenzyl substituted counterparts. All compounds from this series exhibited dual AChE and BuChE inhibition (Table 1). Compound **7g** with a C-4 4-methoxybenzyl substituent was the most potent AChE inhibitor (AChE IC_{50} = 9.40 μM) whereas **7f** (with a C-4 *p*-tolylbenzyl group) was the most potent BuChE inhibitor (BuChE IC_{50} = 2.5 μM, SI = 5.2). All the derivatives (except **7h** and **7i**) exhibited potent BuChE inhibition (IC_{50} = 2.2 μM to 4.9 μM) similar to that of donepezil (IC_{50} = 3.6 μM) and surpassing that of galantamine (IC_{50} = 12.6 μM).

Among **7a**–**j** series, **7e** with a C-4 4-fluorobenzyl substituent was identified as a lead molecule with good AChE/BuChE inhibition and potency (AChE IC_{50} = 7.7 μM, BuChE IC_{50} = 2.2 μM, Table 1).

The ability of a number of pyrimidine-2,4-diamine derivatives to inhibit *h*AChE-induced or self-induced $A\beta_{1-40}$ aggregation was evaluated by a thioflavin T (ThT) fluorescence method and the

Table 1
AChE and BuChE inhibitory activities of pyrimidine-2,4-diamine derivatives (**7a–j**) and their *C*log*P* data along with molecular volumes (MVs)

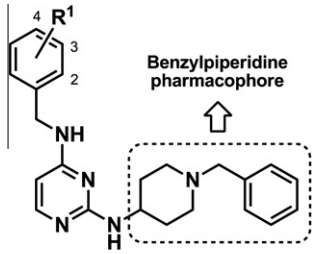

(7a-j)

Compd		R[1]	IC$_{50}$[a] (μM)		SI[b]	*C*log*P*[c]	MV[d]
			AChE	BuChE			
EWGs	**7a**	2-Cl	7.70 ± 0.77	2.40 ± 0.24	3.2	5.32	277.8
	7b	3-Cl	7.70 ± 0.77	2.50 ± 0.23	3.1	5.32	277.8
	7c	4-Cl	8.80 ± 0.88	2.80 ± 0.28	3.1	5.32	277.8
	7d	4-Br	9.90 ± 1.00	4.10 ± 0.40	2.4	5.48	287.1
	7e	4-F	7.70 ± 0.70	2.20 ± 0.20	3.5	4.74	263.1
EDGs	**7f**	4-Me	12.90 ± 0.12	2.50 ± 0.22	5.2	5.10	272.7
	7g	4-OMe	9.40 ± 0.90	4.90 ± 0.50	1.9	4.52	278.8
	7h	3,4-diOMe	9.90 ± 0.99	11.40 ± 0.10	0.9	4.26	299.4
	7i	3,4,5-triOMe	10.30 ± 0.10	7.70 ± 0.65	1.3	3.90	319.3
	7j	3,4-[Dioxole]	12.60 ± 0.12	3.90 ± 0.40	3.2	4.57	280.9
Donepezil (**1**)		—	0.032 ± 0.003	3.60 ± 0.32	—	4.60	271.0
Galantamine (**2**)		—	3.20 ± 0.32	12.60 ± 0.11	0.3	1.0	179.2

[a] The in vitro test compound concentration required to produce 50% inhibition of *h*AChE and *eq*BuChE. The result (IC$_{50}$) is the mean of two separate experiments (n = 4) and the deviation from the mean is <10% of the mean value.
[b] Selectivity Index = *h*AChE/*eq*BuChE IC$_{50}$.
[c] *C*log*P* was determined using ChemDraw Ultra 12.0. CambridgeSoft Company.
[d] Molecular volumes (MV) were calculated after a minimization protocol using the molecular properties calculator in the *Discovery Studio* program from Accelrys Inc (San Diego, CA).

results were compared with reference compounds propidium iodide and donepezil (Table 2).[29] At a concentration of 100 μM, they exhibited varying degrees of inhibition (inactive to 59% inhibition of aggregation). Generally pyrimidine-2,4-diamine derivatives exhibited inhibition of both AChE-induced and self-induced of Aβ_{1-40} aggregation (**7a–j**, Table 2).

In the *h*AChE-induced assay, inhibition ranged from inactive (**7a** and **7c**) up to 59% (**7h**) while in the self-induced assay, inhibition ranged from inactive (**7i**) up to 48% (**7d**). Interestingly, compounds that possessed C-4 EWG group (**7a–e**; Cl, Br or F, respectively) were more effective in the self-induced assay while compounds that possessed C-4 EDGs (**7f–j**; Me, 4-OMe, 3,4-*di*OMe, 3,4,5-*tri*OMe and 3,4-methylenedioxybenzyl) substituted derivatives were more effective in AChE-induced assay. Among these, derivative **7h** was identified as the most effective inhibitor of AChE-induced aggregation (59.3% inhibition, Table 2) and was ~1.3-fold more potent compared to galantamine (48% inhibition). It is plausible that the presence of a C-2 amino-1-benzylpiperidine substituent might play a role in orienting the C-4 3,4-dimethoxybenzyl substituent toward PAS of AChE. It is noteworthy that **7d** (4-bromobenzyl substituent at C-4 position) exhibited dual mode aggregation inhibition in both *h*AChE and self-induced assay (53.90% and 48.40% inhibition, respectively, Table 2).

Lead derivatives from the self-induced assay (**7c** and **7d**, 43.6% and 48.4% inhibition, respectively at 100 μM), were further examined using transmission electron microscopy (TEM) to assess their anti-aggregation activity/morphology in the presence of amyloid peptides (co-incubation, CI assay) and in the presence of preformed amyloid fibrils (pre-fibrillization, PF assay, Fig. 1, Supplementary data). The TEM results confirmed the ability of compounds **7c** (Panel B, Fig. 1, Supplementary data) and **7d** (Panel D, Fig. 1, Supplementary data) to prevent the formation of amyloid fibrils when co-incubated with Aβ_{1-40} peptide compared to control incubation (Panel A, Aβ_{1-40} alone). More significantly, they were also able to dissolve preformed amyloid fibrils when incubated at a concentration of 10 μM (Panels C and E, respectively, Fig. 1, Supplementary data). Over the course of a 6-day co-incubation experiment, both **7c** and **7d** demonstrated anti-aggregation properties similar to that of galantamine (Panel F, Fig. 1, Supplementary data). A three day pre-fibrillization assay prior to test compound incubation both **7c** (Panel C) and **7d** (Panel E) demonstrated their ability to dissolve preformed amyloid fibrils with **7d** exhibiting greater degree of amyloid fibril disassembly relative to **7c**.

The aspartyl protease enzyme BACE-1 is involved in the formation of amyloid-β by cleaving the amyloid precursor protein (APP).[29–31] Recent work from Merck scientists has shown that pyrimidine ring templates could be useful to design potent BACE inhibitors.[31] Since our small molecules are based on a pyrimidine ring scaffold we investigated the ability of BP-derivatives (**7a–j**) to inhibit BACE-1 and results were compared with reference compounds donepezil and the peptide inhibitor *N*-benzyloxycarbonyl-Val-Leu-Leucinal (Table 2).

Activity against β-secretase (IC$_{50}$ values) ranged from 0.6 to >50 μM and was greatly influenced by steric and electronic properties. Derivatives with a C-2 benzylpiperidine pharmacophore generally exhibited potent activity with the exception of **7f** (a *p*-Me

Table 2
Anti-amyloid and BACE-1 inhibition activities of **7a–j**

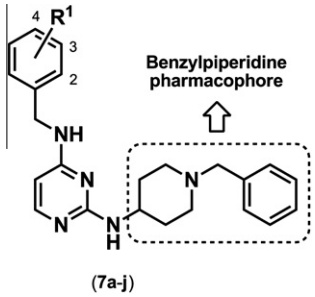

(7a-j)

Compd		R^1	% Inhibition at 100 μM[a]		BACE-1 IC_{50}[b] (μM)
			*h*AChE-induced	Self-induced	
EWGs	**7a**	2-Cl	NA	42.20 ± 0.40	1.70 ± 0.15
	7b	3-Cl	27.20 ± 0.20	39.90 ± 0.35	0.60 ± 0.05
	7c	4-Cl	NA	42.60 ± 0.39	3.20 ± 0.30
	7d	4-Br	53.90 ± 0.45	48.40 ± 0.46	33%[e]
	7e	4-F	38.10 ± 0.33	29.80 ± 0.30	0.70 ± 0.05
EDGs	**7f**	4-Me	45.10 ± 0.45	21.90 ± 0.20	11.10 ± 0.10
	7g	4-OMe	36.20 ± 0.30	18.20 ± 0.20	0.60 ± 0.04
	7h	3,4-diOMe	59.30 ± 0.48	17.40 ± 0.15	34%[e]
	7i	3,4,5-triOMe	32.70 ± 0.30	NA	8.90 ± 0.90
	7j	3,4-[Dioxole]	50.20 ± 0.50	18.60 ± 0.20	1.40 ± 0.13
Donepezil (**1**)		—	17.00[c]	ND	3.20 ± 0.29
Galantamine (**2**)		—	ND	48.00[d]	ND
Propidium		—	82.00	ND	ND
N-Benzyloxycarbonyl-Val-Leu-Leucinal			ND	ND	14.00 ± 0.15

[a] The result (% aggregation inhibition of $A\beta_{1-40}$ at 100 μM) is the mean of two separate experiments ($n = 4$) and the deviation from the mean is <10% of the mean value.
[b] The result (IC_{50}) is the mean of duplicate readings ($n = 2–4$) and the deviation from the mean is <10% of the mean value.
[c] Previously reported (Ref. 23).
[d] Ref. 21. NA = Not active. ND = Not determined.
[e] % BACE-1 inhibition at 10 μM.

benzylamine at C-4) and **7i** (a tri-OMe benzylamine at C-4). When compared to a peptidic BACE-1 inhibitor (*N*-benzyloxycarbonyl-Val-Leu-Leucinal, $IC_{50} = 14.0$ μM), derivatives **7b** (*m*-Cl), **7e** (*p*-F) and **7g** (*p*-OMe) exhibited ~22-fold increase in potency ($IC_{50} = 0.6–0.7$ μM). These studies indicate that a pyrimidine-2.4-diamine based non-peptidic molecules can target BACE-1.

The cytotoxicity of the lead derivative **7h** with multifunctional activities (dual ChE, AChE-induced amyloid aggregation and BACE-1 inhibition) possessing a C-4 3,4-dimethoxybenzyl PAS pharmacophore was evaluated using 3-(4,5-dimethylthiazol-2-yl)-2,5-diphenyl tetrazolium bromide (MTT) based colorimetric assay. Compound **7h** exhibited good cell viability (81%) suggesting that a pyrimidine-2,4-diamine scaffold serves as a suitable template to develop small molecule candidates as multi-targeting agents to treat AD. Furthermore pyrimidine-2,4-diamines (**7a–j**) exhibit *C*log*P* values from 3.90 to 5.48. In this regard, compound **7h** exhibited a *C*log*P* value of 4.26 which compares well with the anti-AD reference agent donepezil (*C*log*P* = 4.60, Table 1) indicating its potential to reach the CNS.

The binding interactions of potent AChE and BuChE inhibitors were investigated by molecular modeling (docking). The most stable enzyme–ligand complex for compound **7e** [N^2-(1-benzylpiperidin-4-yl)-N^4-(4-fluorobenzyl)pyrimidine-2,4-diamine; *h*AChE $IC_{50} = 7.7$ μM) in *h*AChE] (Fig. 2) indicated that the pyrimidine-2,4-diamine template was located at the center of active site gorge (~6.5 Å away from the catalytic triad His447 residue at the bottom of the active site and ~7 Å away from the PAS Trp286). The pyrimidine ring was also oriented between Tyr124 and Tyr337 and was undergoing hydrogen bonding interactions with the tyrosine hydroxyl groups and the C-2 NH and pyrimidine N-3 (distance <3.5 Å). The C-4 group (4-fluorobenzylamine) was oriented such that the fluorine atom was undergoing hydrogen bonding interactions (Asp74 and Asn87; distance ~3.5 Å). This orientation was assisted by Trp86 that was undergoing π–π interactions with the C-4 phenyl ring (distance ~4 Å). The C-2 benzylpiperidine pharmacophore was oriented in a region comprised of Trp286, Tyr341 and Tyr337. Interestingly, the benzyl substituent was positioned at the posterior face of Trp286 (PAS). Overall compound exhibited a linear conformation spanning the catalytic active site (CAS) and PAS which explains its ability to bind to AChE.

Furthermore, the most potent BuChE inhibitor **7e** [N^2-(1-benzylpiperidin-4-yl)-N^4-(4-fluorobenzyl)pyrimidine-2,4-diamine] (*eq*BuChE $IC_{50} = 2.2$ μM) was investigated by docking studies with *h*BuChE (Fig. 3). The most stable enzyme–ligand complex indicates that the pyrimidine-2,4-diamine template was located at the center of the active site gorge (~10 Å away from the catalytic triad His447 residue at the bottom of the active site and ~12 Å away from the entry site residue, Ala277). Similar to its *h*AChE binding mode, the entire C-4 group (4-fluorobenzylamine) was oriented such that the fluorine atom toward His438 (hydrogen bonding interaction; distance ~3.5 Å) and Ser198. The C-2 benzylpiperidine pharmacophore was oriented in a hydrophobic region alongside Pro285 and acyl pocket (Leu286, Ser287, Val288; distances ~4–5 Å) with the phenyl ring was about ~4 Å away from Trp231 and Phe398. It was interesting to note that **7e** (molecular volume 263.1 $Å^3$) was oriented in an inverse U-shaped conformation and was able to interact with key residues within the active site of BuChE.

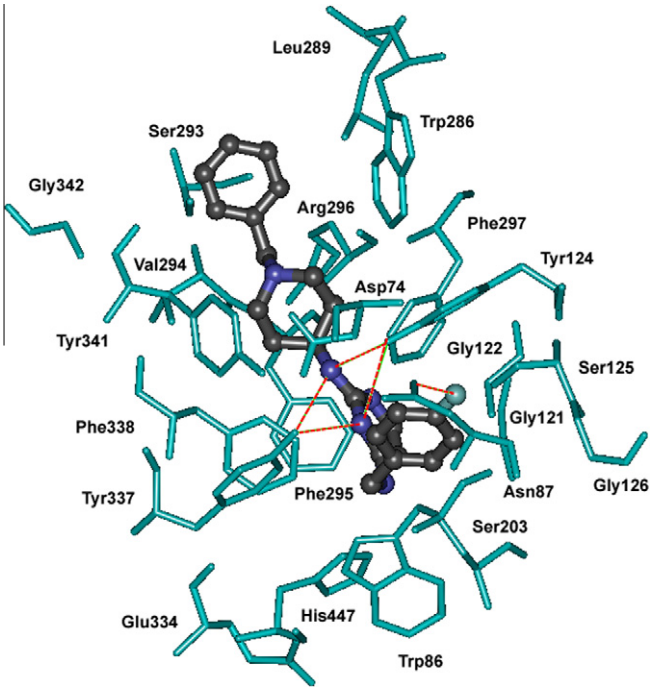

Figure 2. The binding mode of N^2-(1-benzylpiperidin-4-yl)-N^4-(4-fluorobenzyl)pyrimidine-2,4-diamine (**7e**, ball and stick) in *h*AChE (PDB: 1B41). Red dotted lines indicate hydrogen bonding interactions. Hydrogen atoms are removed to increase clarity.

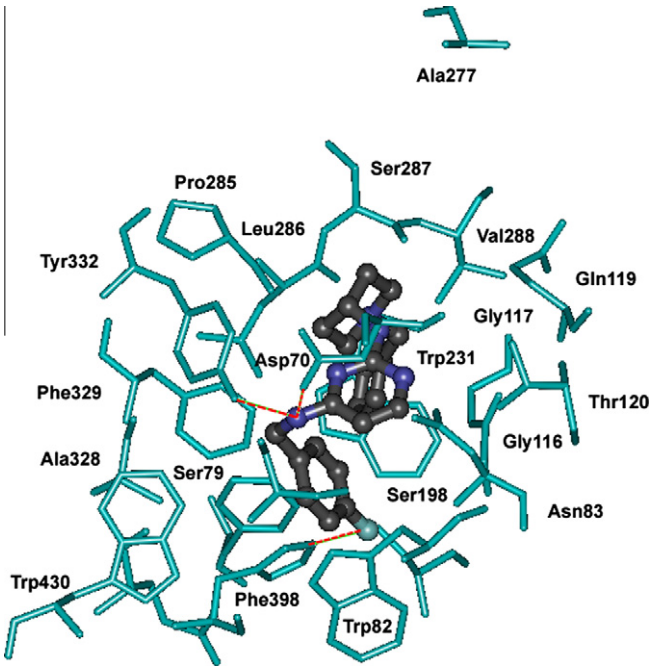

Figure 3. The binding mode of N^2-(1-benzylpiperidin-4-yl)-N^4-(4-fluorobenzyl)pyrimidine-2,4-diamine (**7e**, ball and stick) in *h*BuChE (PDB: 1P0I). Red dotted lines indicate hydrogen bonding interactions. Hydrogen atoms are removed to increase clarity.

In order to understand the binding mode of compound **7h** [N^2-(1-benzylpiperidin-4-yl)-N^4-(3,4-dimethoxybenzyl)pyrimidine-2,4-diamine] that exhibited good inhibition of AChE-induced Aβ-aggregation (59% inhibition, Table 2), it was docked within the active site of *h*AChE and was compared with the binding mode of reference agent donepezil that is known to orient the 3,4-dimethoxy group closer to AChE–PAS (Fig. 4). It should be noted that the compound **7h** (molecular volume = 299.4 Å^3, Table 1) is much larger as compared to donepezil (molecular volume = 271 Å^3). This investigation shows that the C-4 3,4-dimethoxybenzylamine substituent of **7h** was much closer to the PAS residues (distance ~4 Å) compared to donepezil and was tightly stacked against the indole ring of Trp286 correlating with its superior activity against AChE-induced Aβ-aggregation compared to donepezil (59% vs 17% at 100 μM). In this regard, a C-4 3,4-dimethoxybenzyl substituent could be considered as a suitable PAS binding pharmacophore in the development of novel pyrimidin-2,4-diamine based small molecules.

The SAR data obtained from this pyrimidin-2,4-diamine chemical library indicates that steric and electronic properties at C-4 position exert a significant effect on the AChE, BuChE, β-amyloid and BACE-1 inhibitory profiles. In this regard, a C-2 amino-1-benzylpiperidine was identified as a dual ChE binding pharmacophore whereas a C-4 3,4-dimethoxybenzyl substituent was identified as a PAS binding pharmacophore capable of inhibiting AChE-induced amyloid aggregation. From our library, compound **7e** [N^2-(1-benzylpiperidin-4-yl)-N^4-(4-fluorobenzyl)pyrimidine-2,4-diamine] was identified as the most potent dual ChE inhibitor (AChE IC_{50} = 7.7 μM; BuChE IC_{50} = 2.2 μM) whereas **7d** [N^2-(1-benzylpiperidin-4-yl)-N^4-(4-bromobenzyl)pyrimidine-2,4-diamine] exhibited potent β-amyloid aggregation inhibition (AChE-induced = 53.9%; self-induced = 48.4% at 100 μM). In addition, **7h** [N^2-(1-benzylpiperidin-4-yl)-N^4-(3,4-dimethoxybenzyl)pyrimidine-2,4-diamine] was identified as a promising small molecule with multifunctional anti-AD profile (IC_{50}: *h*AChE = 9.9 μM, *eq*BuChE = 11.4 μM; *h*AChE-induced $A\beta_{40}$-aggregation inhibition = 59.3% at 100 μM; self-induced $A\beta_{40}$-aggregation inhibition = 17.4% at 100 μM[32–34] and BACE-1 = 34% inhibition at 10 μM) with good cell viability in the SH-SY5Y neuroblastoma cell line (81%).[35,36] Together, these results imply that pyrimidin-2,4-diamines are suitable ring templates to design anti-AD small molecule therapeutics as disease-modifying agents (DMAs).

Acknowledgments

The authors would like to thank Faculty of Science and the School of Pharmacy at the University of Waterloo for financial support of this research project.

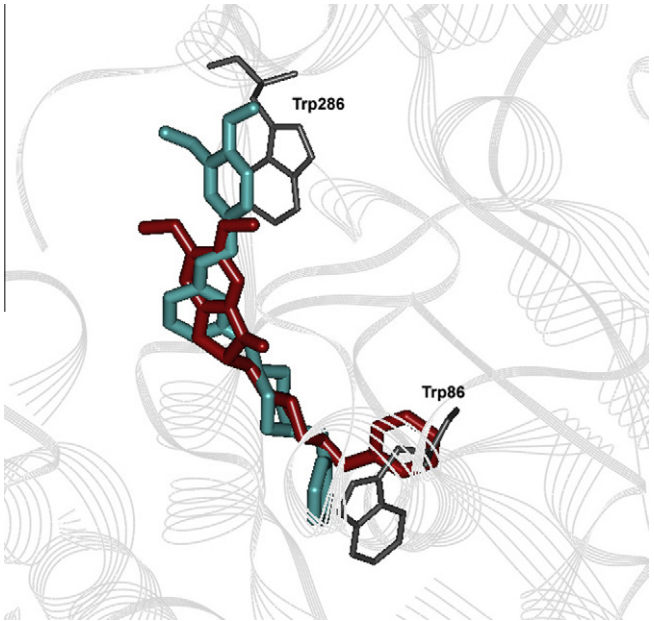

Figure 4. Superimposition of docked structures comparing the binding modes of N^2-(1-benzylpiperidin-4-yl)-N^4-(3,4-dimethoxybenzyl)pyrimidine-2,4-diamine (**7h**, Green) with that of donepezil (*R*ed, **1**, Fig. 1) in *h*AChE (PDB: 1B41).

Supplementary data

Supplementary data associated with this article can be found, in the online version, at http://dx.doi.org/10.1016/j.bmcl.2012.05.077.

Reference and notes

1. Holden, M.; Kelly, C. *Adv. Psychiatr. Treat.* **2002**, *8*, 89.
2. Klafki, H.; Staufenbiel, M.; Kornhuber, J.; Wiltfang, J. *Brain* **2006**, *129*, 2840.
3. Edwards, P. D.; Albert, J. S.; Sylvester, M.; Aharony, D.; Andisik, D.; Callaghan, O.; Campbell, J. B.; Carr, R. A.; Chessari, G.; Congreve, M.; Frederickson, M.; Folmer, R. H. A.; Geschwindner, S.; Koether, G.; Kolmodin, K.; Krumrine, J.; Mauger, R. C.; Murray, C. W.; Olsson, L.; Patel, S.; Spear, N.; Tian, G. *J. Med. Chem.* **2007**, *50*, 5912.
4. Selkoe, D. J. *Science* **2002**, *298*, 789.
5. Aguzzi, A.; O'Conner, T. *Nat. Rev. Drug Disc.* **2010**, *9*, 237.
6. Melnikova, I. *Nat. Rev. Drug Disc.* **2007**, *6*, 341.
7. Suh, W. H.; Suslick, K. S.; Suh, Y. *Curr. Med. Chem.* **2005**, *5*, 259.
8. Shen, T.; Tai, K.; Henchman, R. H.; McCammon, J. A. *Acc. Chem. Res.* **2002**, *35*, 332.
9. Darvesh, S.; Hopkins, D. A.; Geula, C. *Nat. Rev. Neurosci.* **2003**, *4*, 131.
10. Kamal, M. A.; Qu, X.; Yu, Q.; Tweedie, D.; Holloway, H. W.; Li, Y.; Tan, Y.; Greig, N. H. *J. Neural Transm.* **2008**, *115*, 889.
11. Campiani, G.; Fattorusso, C.; Butini, S.; Gaeta, A.; Agnusdei, M.; Gemma, S.; Persico, M.; Catalanotti, B.; Savini, L.; Nacci, V.; Novellino, E.; Holloway, H. W.; Greig, N. H.; Belinskaya, T.; Fedorko, J. M.; Saxena, A. *J. Med. Chem.* **1919**, *2005*, 48.
12. Gibbs, M. E.; Maksel, D.; Gibbs, Z.; Hou, X.; Summers, R. J.; Small, D. H. *Neurobiol. Aging* **2010**, *31*, 614.
13. Dinamarca, M. C.; Sagal, J. P.; Quintanilla, R. A.; Godoy, J. A.; Arrazola, M. S.; Inestrosa, N. C. *Mol. Neurodegener.* **2010**, *5*, 2.
14. Rosini, M.; Simoni, E.; Bartolini, M.; Cavalli, A.; Ceccarini, L.; Pascu, N.; McClymont, D. W.; Tarozzi, A.; Bolognesi, M. L.; Minarini, A.; Tumiatti, V.; Andrisano, V.; Mellor, I. R.; Melchiorre, C. *J. Med. Chem.* **2008**, *51*, 4381.
15. Pakaski, M.; Kalman, J. *Neurochem. Int.* **2008**, *53*, 103.
16. Racchi, M.; Mazzucchelli, M.; Lenzken, S. C.; Porrello, E.; Lanni, C.; Govoni, S. *Chem. Biol. Interact.* **2005**, *157–158*, 335.
17. Inestrosa, N. C.; Dinamarca, M. C.; Alvarez, A. *FEBS* **2008**, *275*, 625.
18. Inestrosa, N. C.; Alvarez, A.; Perez, C. A.; Moreno, R. D.; Vincete, M.; Linker, C.; Casanueva, O. I.; Soto, C.; Garrido, J. *Neuron* **1996**, *16*, 881.
19. Belluti, F.; Rampa, A.; Piazzi, L.; Bisi, A.; Gobbi, S.; Bartolini, M.; Andrisano, V.; Cavalli, A.; Recanatini, M.; Valenti, P. *J. Med. Chem.* **2005**, *48*, 4444.
20. Terry, A. V., Jr.; Callahan, P. M.; Hall, B.; Webster, S. J. *Behaviour* **2011**, *99*, 190.
21. Matharu, B.; Gibson, G.; Parsons, R.; Huckerby, T. N.; Moore, S. A.; Cooper, L. J.; Millichamp, R.; Allsop, D.; Austen, B. *J. Neurol. Sci.* **2009**, *280*, 49.
22. Mohamed, T.; Rao, P. P. N. *Curr. Med. Chem.* **2011**, *18*, 4299.
23. Mohamed, T.; Zhao, X.; Habib, L. K.; Yang, J.; Rao, P. P. N. *Bioorg. Med. Chem.* **2011**, *19*, 2269.
24. Mohamed, T.; Yeung, J. C. K.; Rao, P. P. N. *Bioorg. Med. Chem. Lett.* **2011**, *21*, 5881.
25. Nugiel, D. A.; Cornelius, L. A. M.; Corbett, J. W. *J. Org. Chem.* **1997**, *62*, 201.
26. Fiorini, M. T.; Abell, C. *Tetrahedron Lett.* **1827**, *1998*, 39.
27. Ellman, G. L.; Courtney, K. D.; Andres, V., Jr.; Featherstone, R. M. *Biochem. Pharmacol.* **1961**, *7*, 88.
28. Alvarez, A.; Alarcon, R.; Opazo, C.; Campos, E. O.; Munoz, J.; Calderon, F. H.; Dajas, F.; Gentry, M. K.; Doctor, B. P.; De Mello, F. G.; Inestrosa, N. C. *J. Neurosci.* **1998**, *18*, 3213.
29. Stachel, S. J. *Drug Dev. Res.* **2009**, *70*, 101.
30. Citron, M. *Nat. Rev. Drug Disc.* **2010**, *9*, 387.
31. Steele, T. G.; Hills, I. D.; Nomland, A. A.; de Leon, P.; Allison, T.; McGaughey, G.; Colussi, D.; Tugusheva, K.; Hauqabook, S. J.; Espeseth, A. S.; Zuck, P.; Graham, S. L.; Stachel, S. J. *Bioorg. Med. Chem. Lett.* **2009**, *19*, 17.
32. Zhao, X.; Yang, J. *ACS Chem. Neurosci.* **2010**, *1*, 665.
33. Khurana, R.; Coleman, C.; Ionescu-Zanetti, C.; Carter, S. A.; Krishna, V.; Grover, R. K.; Roy, R.; Singh, S. *J. Struc. Biol.* **2005**, *151*, 229.
34. Eubanks, L. M.; Rogers, C. J.; Beuscher, A. E., IV; Koob, G. F.; Olson, A. J.; Dickerson, T. J.; Janda, K. D. *Mol. Pharm.* **2006**, *3*, 773.
35. Mosmann, T. *J. Immunol. Methods* **1983**, *65*, 55.
36. Vellonen, K.; Honkakoski, P.; Urtti, A. *Eur. J. Pharm. Sci.* **2004**, *23*, 181.